Torque-control based compliant actuation of a quadruped robot

Article · March 2012

DOI: 10.1109/AMC.2012.6197133

CITATIONS
19

READS
1,109

6 authors, including:

Michele Focchi
Università degli Studi di Trento
74 PUBLICATIONS **2,640** CITATIONS
SEE PROFILE

Thiago Boaventura
ETH Zurich
26 PUBLICATIONS **682** CITATIONS
SEE PROFILE

Claudio Semini
Istituto Italiano di Tecnologia
146 PUBLICATIONS **4,154** CITATIONS
SEE PROFILE

Torque-control Based Compliant Actuation of a Quadruped Robot

Michele Focchi, Thiago Boaventura, Claudio Semini, Marco Frigerio, Jonas Buchli, Darwin G. Caldwell

Department of Advanced Robotics, Istituto Italiano di Tecnologia (IIT)
Email: {michele.focchi, thiago.boaventura, claudio.semini, marco.frigerio, jonas.buchli, darwin.caldwell}@iit.it

***Abstract*— In the realm of legged locomotion, being compliant to external unperceived impacts is crucial when negotiating unstructured terrain. Impedance control is a useful framework to allow the robot to follow reference trajectories and, at the same time, handle external disturbances. To implement impedance control, high performance torque control in all joints is of great importance. In this paper, the torque control for the electric joints of the HyQ robot is described and its performance assessed. HyQ is a quadruped robot which has hybrid actuation: hydraulic and electric. This work complements our previous work, in which the torque control for the hydraulic joints was addressed. Subsequently, we describe the implementation of an impedance controller for the HyQ leg. Experimental results assess the tracking capability of a desired Cartesian force at the end-effector under the action of external disturbances. Another set of experiments involves the tracking and the shaping of different desired stiffness behaviors (stiffness ellipses) at the foot.**

I. Introduction

Today the majority of legged robots employ high gain position error feedback control. Such robots exhibit a very stiff disturbance rejection behavior and are therefore not well suited to deal with unstructured environments as presented by the real world outside the laboratory. To achieve robust robotic legged locomotion over unstructured, difficult and partially unknown terrains, different control approaches are required.

Trajectory tracking is needed when there is no physical interaction of the robot with the environment (e.g. moving the swing leg in the air as fast and precise as possible to place accurate footsteps). At the same time, the control of the dynamic behavior of the foot in case of physical interaction is desirable. It allows, for example, to behave either compliantly, in case the robot hits an obstacle, or stiffly, in case it has to position an object. A controller that is able to deal with all these situations is of paramount importance for a proper overall robot behavior.

A possible solution to improve the robustness of legged locomotion is to be able to tune the compliance of the legs according to the task that must be executed. A trivial way would be to reduce the *joint* position controller gains at the cost of inferior tracking accuracy. Previous works [3] show that, for a mobile articulated robot, a way to obtain compliance without sacrificing accuracy is to use floating-base inverse dynamics control. This type of control is able to predict the required torque based on the robot rigid body dynamics model. It leads to more robust locomotion in case of ill-perceived terrain. While the inverse dynamics helps to improve tracking, the use of joint space position control to stabilize the motion leads to an end-effector impedance that is configuration dependent and therefore also non-constant. It would be more convenient to be able to specify the impedance independently of the configuration.

Therefore, alternatively, we can integrate the above requirements in an appropriate impedance behavior and use a customized impedance controller defined in the *end-effector space*. In a simple implementation, also no explicit measurement of the interaction force is required. This alternative is the one followed in this paper.

Impedance control is a suitable framework to control robots in contact with unknown environments [7], as it is the case for legged locomotion over rough terrains. The underlying idea of impedance control is to design a disturbance response for deviation from the prescribed motion which has the form of an impedance. In other words, we want to be able to define a desired end-effector dynamic behavior. The interaction between manipulator and environment may be modulated by changing end-effector impedance (i.e. its inertia, damping and stiffness defined in the end-effector space) while the environment is regarded as a source of disturbances.

A well established framework for impedance control was introduced by Hogan [7]. In the last decade, thanks to the availability of accurate torque sensors on the joints, this has been extensively implemented. In [1] an overview of different controller architectures (impedance together with admittance control and stiffness control) is also given. Active compliance is not a new topic for legged robots. In the DLR crawler hexapod, an active compliance controller has been implemented at joint level [6], similarly to what has been done in [13] for multi-DoF bipedal walking. Generalizing the previous idea, we can state that a desired impedance can be set to any point of the robot, given a kinematic transformation between this point and the actuated joint variables exists. It opens a wide range of applications, like the possibility to define an impedance behavior for the COG, and to employ the concepts of the framework of virtual mode control [9].

The presence of an impedance control permits also to easily adjust the robot impedance behavior depending on its needs. It is possible, for instance, to ”shape” spatially the overall robot stiffness characteristics (e.g. set a certain stiffness ellipsoid). A practical example would be to increase the stiffness of the leg in the transversal and vertical direction (to be able to

maintain the posture) while keeping it compliant in the forward direction (for dealing with impacts and obstacles). Being able to change the impedance in real-time is a desired capability when dealing with very dynamic motions (e.g.running). This on-the-fly adaptation is present in animal locomotion, where the leg impedance is chosen according to the terrain stiffness in order to keep the motion profile of the center of mass constant [4].

The experimental platform used for the project is the quadruped robot HyQ [12] (Fig.1). In this work we present the implementation of an impedance controller, as described by Hogan [7], to control the 3 DOF electro-hydraulically driven leg of HyQ. We demonstrate through simulation and experimental data that this controller is able to generate Cartesian force vectors at the end effector. Moreover, we show in this work the torque controller formulation and implementation for the electrical joints. This completes the work done in [2], in which the torque controller for the hydraulic joints is described. The presence of a high-fidelity torque source allowed us to straightforwardly implement a proper impedance control. In this work, the base frame of the leg is considered fixed to the ground.

The paper is structured as follows: in Section II, the HyQ platform and the mechanical structure of the hip abduction/adduction joint will be briefly described. The controller design and performances are presented in Section III. Next, Section IV presents the impedance controller design. In Section V experimental results with the impedance controller are shown before concluding the paper with a discussion of the results and an outlook in Section VI.

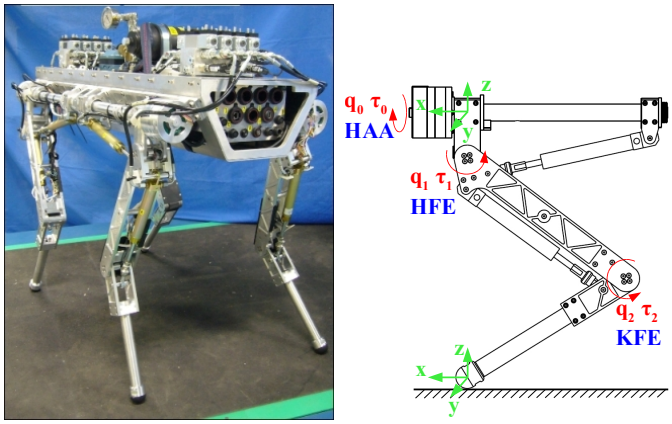

Fig. 1. HyQ: Hydraulic Quadruped robot. **Left:** picture of the robot. **Right:** sketch with labels of the three leg joints, hip abduction/adduction (HAA), hip flexion/extension (HFE) and knee flexion/extension (KFE)

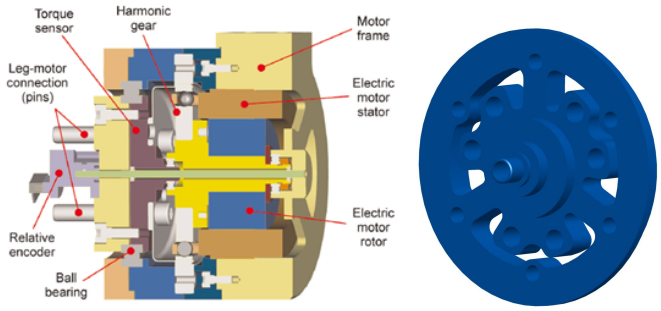

Fig. 2. **Left:** Electric motor assembly: cross-section of the CAD model. **Right:** Torque sensor CAD model.

II. HyQ

Our experimental research platform *HyQ* has 12 active degrees of freedom (DOF). Each leg features three actuated revolute DOF, which is the minimum required to allow a foot positioning in a three-dimensional workspace (Fig. 1). The hip abduction/adduction (HAA) joints are driven by brushless DC electric motors and connect the legs to the robot torso, creating the lateral leg motion. The hip and knee flexion/extension (HFE and KFE, respectively) are actuated by hydraulic cylinders, which are driven by high performance servo-valves (bandwidth around 250Hz) [8]. Position sensing is performed by absolute and relative encoders on each joint, while torque sensing is obtained by custom-designed torque sensors (HAA) and load cells (HFE ,KFE). As this paper focuses on the torque control of the HAA joint, we will now introduce the design of the electric motor unit and torque sensor. Further details of the robot design and selection of actuator types can be found in [11] and [12]. As shown in Fig. 2, a frame-less brush-less motor consisting of stator and rotor is inserted into a custom-made motor frame, which is mounted onto the robot torso. The rotor is solidly interconnected with the harmonic gear train (reduction ratio 1:100) that transfers the movement to the HAA joint creating the abduction/adduction movement of the leg. A custom-designed torque sensor (Fig. 2) is placed right after the harmonic gear to measure the link torque. The design of this torque sensor is based on a similar strain gage sensor presented in [14]. It has been optimized to match the peak output torque of the electric motor (140Nm at 48V after gear reduction) and momentary peak torque of the harmonic gear (152Nm), while maximizing sensitivity. Absolute and relative encoder are placed both link-side. We use high resolution relative encoders (80000 counts per revolution) to reduce quantization errors in link velocity calculation.

III. Leg control overview and torque controller

In this section we first give an overview of the control architecture of the leg then focus on the torque controller of the HAA joint. As shown in the block diagram (Fig. 3) the core elements of the control architecture are the inner torque loops of the three joints. In this work the outer loop is an impedance controller defined in the task space. The outputs of the outer loop are the torque references (τ^{ref}) that are fed to the three inner joint torque controllers. The torque control loops relative to the hydraulic joints (HFE and KFE) (described in [2]) generate commands for the valves u_v, while the one relative to the electrical HAA joint generates a PWM command for the motors u_m. All the control loops run on a PC104 stack with Pentium CPU board. The torque loops rate is 1kHz rate while the outer impedance controller runs at 200Hz.

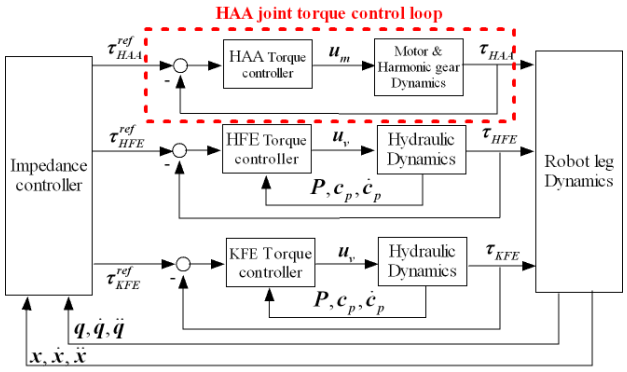

Fig. 3. Block diagram of the Leg control architecture

HAA torque controller - For our torque controller a simple PI scheme (P=1 V/Nm, I=40 V/Nms) seems to work satisfactorily. To prevent performance reduction due to the integral term in case of actuator saturation, a classical anti-windup scheme has been implemented [5]. The torque control performance was assessed via a 10 Nm step response (with the HAA joint fixed), see Fig. 4. Experimental results show a rise time t_r of 32ms. Closed loop bandwidth is estimated to be around 10Hz (considering a rough approximation to a 1^{st} order dynamics $t_r = 0.35/BW$) [5].

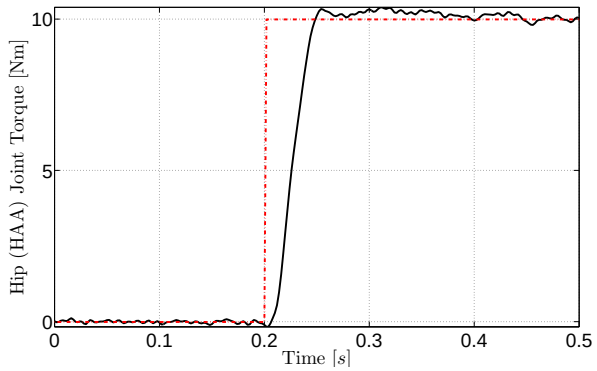

Fig. 4. Torque step at the hip HAA joint (fixed leg): the dashed line is the torque reference and the solid black the measured torque

Then a closed loop PD position control loop with an Inverse Dynamics feedforward torque (P=600, D=10) for the hip (HAA) angular position has been closed around the torque controller (the gains are expressed in SI units, and thus correspond to 600Nm/rad stiffness and 10 Nms/rad damping in the joint coordinate). Subsequently, a 0.2 rad - 1.5Hz sinusoidal reference has been set with a 0.1 rad offset about the vertical position. The leg was set in a stretched configuration as depicted in Fig.1. A 5 kg mass was attached at the end-tip to have a significant load. The tracking performance is shown in Fig. 5, both for the position and the torque. The leg was randomly perturbed between 1s and 2.3s. The torque controller reacts promptly to this disturbance and this creates an error in the position loop proportional to the disturbance force as expected from a linear impedance. This proportionality is only qualitative because the sensor measurement does not discriminate between actuator torques and disturbance torques.

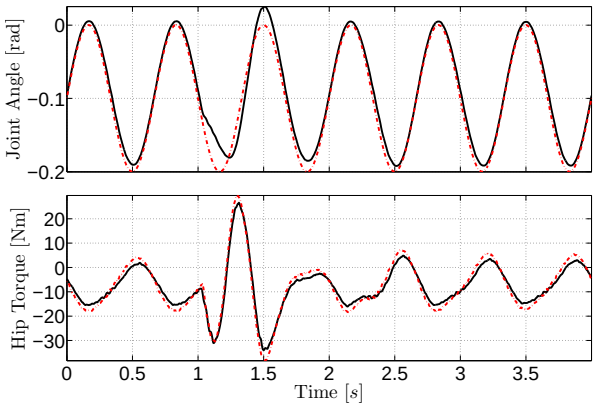

Fig. 5. Position and torque tracking for a 0.2 rad - 1.5 Hz sine position reference trajectory for the hip (HAA) joint. The dashed line indicates the reference signals and the black solid one the actual values

IV. 3D IMPEDANCE CONTROLLER

The goal of an end-effector Cartesian impedance controller is to define a dynamic relationship between the Cartesian position x of the end-effector (i.e. the foot of the robot) and the Cartesian forces F_{ext}. The following theory is well known and is included for the sake of completeness.

A common choice for the impedance behavior is a dynamical system of second order in which we can identify a Cartesian inertia M_x, a damping D_x, and a stiffness K_x:

$$F_{ext} = K_x(x - x_0) + D_x(\dot{x} - \dot{x_0}) + M_x\ddot{x} \qquad (1)$$

where x is the actual Cartesian position and x_0 is the desired position. In our case since, since we have a 3DOF leg and we are not controlling foot orientation, M_x, D_x and K_x will be 3×3 matrices.

To implement the target behavior defined in Eq. (1), we express the desired Cartesian coordinate impedance in actuator coordinates and then use a model of the manipulator dynamics to derive the required controller equations [7] as follows. First, the desired behavior expressed in (1) can be rearranged into a specification of the desired end-point acceleration, which is the result of an external force F_{ext} applied on the manipulator:

$$\ddot{x_d} = {M_x}^{-1}\left[-K_x(x - x_0) - D_x(\dot{x} - \dot{x}_0) + F_{ext}\right] \qquad (2)$$

We now need to find the joint torques that realize the specified acceleration. To do so, we must relate the end-effector position and acceleration to joint space coordinates by the known relationships [10]:

$$\begin{aligned} \dot{x} &= J(q)\dot{q} \\ \ddot{x} &= J(q)\ddot{q} + \dot{J}\dot{q} \\ \ddot{q} &= J^{-1}\left(\ddot{x} - \dot{J}\dot{q}\right) \end{aligned} \qquad (3)$$

where J is the Jacobian that relates the end-effector motion to the joint motion, and q is the joint configuration of the leg. Then, by plugging (2) into (3), we can obtain the vector of joint accelerations necessary to obtain the desired impedance in the Cartesian space:

$$\ddot{q_d} = J^{-1}(M_x^{-1}[-K_x(x - x_0) + \\ - D_x(\dot{x} - \dot{x}_0) + F_{ext}] - \dot{J}\dot{q}) \tag{4}$$

Now we consider a model of the manipulator dynamics as follows:

$$\tau^{ref} + J^T F_{ext} = M_j\ddot{q} + C_j\dot{q} + G_j \tag{5}$$

where M_j, C_j and G_j are the inertia, centripetal-Coriolis, and gravity matrix respectively, while τ^{ref} is the computed reference sent to the inner joint torque loops. $J^T F_{ext}$ is a vector of external torques, which represents the interaction of the robot with its environment. It is important to underline that M_j, C_j and G_j are dependent on the joint configuration while M_x, D_x and K_x are constant.

By plugging (4) into (5), we can find joint torques that compensate for manipulator dynamics and realize the desired impedance in the Cartesian space [7]:

$$\tau^{ref} = M_j J^{-1}\{M_x^{-1}[-K_x(\kappa(q) - x_0) - D_x(J\dot{q} - \dot{x}_0) + \\ F_{ext}] - \dot{J}\dot{q}\} - J^T F_{ext} + C_j\dot{q} + G_j \tag{6}$$

From Eq. (6), it can be seen that the dynamics of the robot and of the end-effector are strongly coupled. Desired passive impedance can be chosen by having M_x, D_x and K_x as symmetric, positive definite matrices. It is possible to choose the directions in which to set the maximum/minimum stiffness/damping/inertia by selecting the eigenvectors of these matrices. If we choose them diagonal, we can set impedance along the directions of the coordinate frame w.r.t the end-effector position. By this way, the end-effector inertia (in the x,y, z directions), in the response to an external disturbance, will be represented by the m_{11}, m_{22}, m_{33}, respectively. It is really important to underline that to achieve a correct decoupling in the Cartesian space (e.g. to avoid that an external force in the x direction cause a movement in z and y direction other than in x), it is necessary to compensate for the interaction forces in the joint space ($J^T F_{ext}$) while accounting for their Cartesian measures F_{ext} in the impedance equation (1). A distal force sensor is necessary to measure these forces because an estimate made by the force sensors at joint level will be accounting also for gravity and robot inertial forces. Therefore, for this control scheme a 3-axis force sensor is needed, placed right at the point where the impedance behavior is desired (in our case the foot).

To assess the correctness of this controller, a simulation that considers the leg in the default configuration (depicted in the sketch of Fig. 1) is made. We set a diagonal stiffness, damping and inertia matrix with diagonal elements that are equals to $k_{ii} = 400N/m$, $d_{ii} = 20N/m$ and $m_{ii} = 1kg$ respectively. $m_{ii} = 1kg$ means that the end effector should behave as a 1 kg mass in all directions. Applying an external step force disturbance $F_{ext} = [30, 60, 0]N$ to the foot, we obtain the following result (Fig.6):

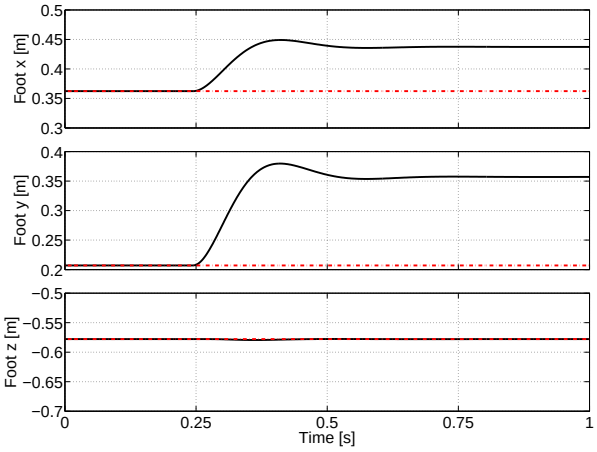

Fig. 6. Deflection of the foot position (solid back line) from the reference position (dashed line) in consequence of a $F_{ext} = [30, 60, 0]N$ step external force acting at 0.25s. The first plot refers to the x component(sagittal), the second to the y (transversal) and the third to the z (vertical) in the coordinate frame

Having M_x, D_x and K_x as diagonal matrices implies that a force disturbance in the plane x-y will result in a deflection in the same plane, with no movement in the z direction. Fig. 6 shows a deflection of 0.075 m and 0.15m in x and y direction, respectively, while zero in the z direction. This is coherent with the application of a force of 30N and 60N in the x and y direction with to a system with the stiffness of $k_{ii} = 400N/m$. We can verify that the dynamic behavior is the one expected by looking at the 95% settling time of the end-effector dynamics, that is imposed to be of the 2^{nd} order. As known [5], for a 2^{nd} order system the settling time t_s is related to the natural frequency ω and damping ε as $t_s \simeq 2.3/\varepsilon\omega_n$. For an impedance defined as (1), we have $\varepsilon = d_{ii}/2\sqrt{k_{ii}m_{ii}}$ and $\omega_n = \sqrt{k_{ii}/m_{ii}}$. Therefore, by substituting the previous values for k_{ii}, d_{ii} and m_{ii}, we obtain a settling time of $t_s = 0.23s$. This matches the settling time in the simulation of Fig. 6, demonstrating that the impedance behavior set by the controller is correct.

The impedance controller in Eq. (6) can be simplified if a change of in the end-effector inertia is not required and we do not wish to compensate for gravity and Coriolis/Centripetal forces. In this case, the controller would create only a virtual spring-damper attaching the end-effector to its desired trajectory. The advantage of this approach is that it does not require a measurement of the interaction forces at the end-effector. Since the design of a 3-axis foot sensor is still part of a ongoing work, this simpler approach will be implemented in the experiments, leaving the implementation of the full impedance controller (6) for future work.

The idea of the simpler approach is that, whenever an external disturbance creates a deflection of the actual end-effector position x w.r.t. the desired equilibrium point x_d, the

manipulator creates forces F in the Cartesian space that are a function of this deflection and of its derivative:

$$F = -K_x(x - x_0) - D_x(\dot{x} - \dot{x}_0) \tag{7}$$

To generate forces at the end-effector, we need to apply torques at the joints. By using the transposed Jacobian, we can convert these Cartesian forces into desired joint torques:

$$\tau^{ref} = J^T \left[-K_x(x - x_0) - D_x(\dot{x} - \dot{x}_0)\right] \tag{8}$$

All the Cartesian forces can be mapped into the joint space with the Jacobian transpose. It is important to remark that, even if the equations (8) and (6) require the inverse or the transpose Jacobian, they do not require inversion of the kinematics equations. Only forward kinematic equations need to be computed. Therefore, this approach can be easily extended to a manipulator with kinematic redundancies for which no closed form solution of the inverse kinematic equations exists [7]. Furthermore, this framework can be extended to any point of the robot (e.g. the COG) following the same recipe and using as Jacobian the one that defines the movement of that point w.r.t the joint variables. Another advantage of impedance control is that the stability is preserved also in case of singularities [1]. In Eq. (8), gravity is considered as an external force, creating offset values on the 3 components of F. It becomes more evident when a low stiffness is set.

V. Experiments

In the experiments, we will consider the leg only as a fixed base system. A full floating base treatment will be part of future works. As mentioned in the previous section, the impedance controller has been implemented in its simpler form (8). Damping and stiffness matrices, D_x and K_x, are selected to be positive definite diagonal matrices with diagonal elements set to $d_{ii} = 20N/(m/s)$ and $k_{ii} = 400N/m$, respectively. A smoothing spline algorithm is applied whenever an impedance parameter or a reference parameter is changed to prevent torque discontinuities and to avoid triggering instabilities.

A. Force tracking in the task space

To assess the force tracking in the end-effector space, we set the desired position to be constant. Random disturbance forces are applied by the user at the end-effector in different directions. Because of these disturbances, reference forces are generated by the impedance controller. We repeated the test in different foot locations inside a 16cm-side cubic workspace centered around the default leg configuration (depicted in the sketch of Fig. 1). We obtained similar tracking results for different foot locations, thus we show only the time history relative to one of them in Fig. 7.

An FFT of the signals shows that the applied disturbance has a bandwidth limited to 3 Hz. The RMS of the Euclidean norm of the tracking error (shown in the bottom plot of 7) is around 4.5N, while the maximum end-effector force (norm) is 60N. The figure shows that the force is properly tracked at the end-effector space and that the controller is able to deal satisfactorily with low frequency ($< 3Hz$) random disturbances in the range of 60N.

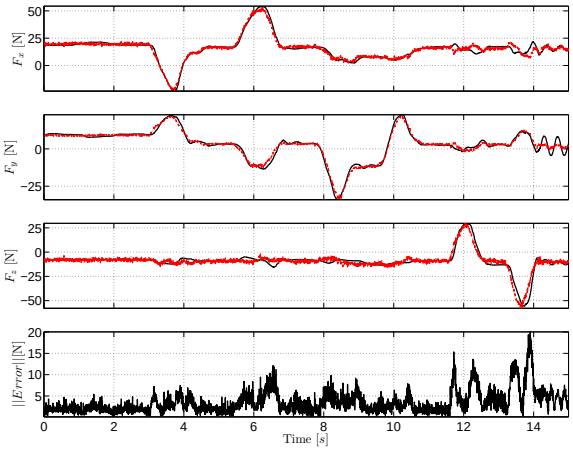

Fig. 7. Time plot of end-effector force tracking in the foot coordinate frame: reference Cartesian force (dashed line) and measured end-effector force (solid back line)(estimated by joint torques). 4th plot represents the Euclidean norm of the force tracking. error

B. Stiffness ellipse in the x-y plane

A way to demonstrate that forces generated at the foot are coherent with the desired impedance behavior is showing how the controller is able to track a desired stiffness ellipse. For the sake of simplicity, we constrained this experiment only to the x-y plane, but this can easily be extended to the 3D space. In this test, the foot desired position is kept constant while a user was moving the foot on a circular path on the x-y plane. By simple vectorial algebra computations, it is possible to assess the stiffness ellipse in this plane. The first two parameters (K_{xx} and K_{yy}) of the diagonal of the stiffness matrix (that define the stiffness shape in the x-y plane) have been set to test different shapes of the stiffness ellipse, according to Table. I.

TABLE I
Stiffness ellipse

Ellipse Shape	$K_{xx}[N/m]$	$K_{yy}[N/m]$
Shape 1	300	300
Shape 2	150	400
Shape 3	400	150

In particular, the left plot of Fig. 8 shows a configuration in which the values are equal (shape 1) and the stiffness ellipse becomes a circle. In the right and bottom plots, a stiffness ellipses is represented in which the stiffer direction is y (shape 2) and x (shape 3) respectively. The plots in Fig. 8 demonstrate the effective versatility of the implemented controller in shaping the stiffness behavior at the end-effector.

VI. Conclusions and Future Work

In this work, we described a torque controller for the hip electric joint (HAA) of the HyQ leg assessed its performance. The maximum closed loop bandwidth (with the leg

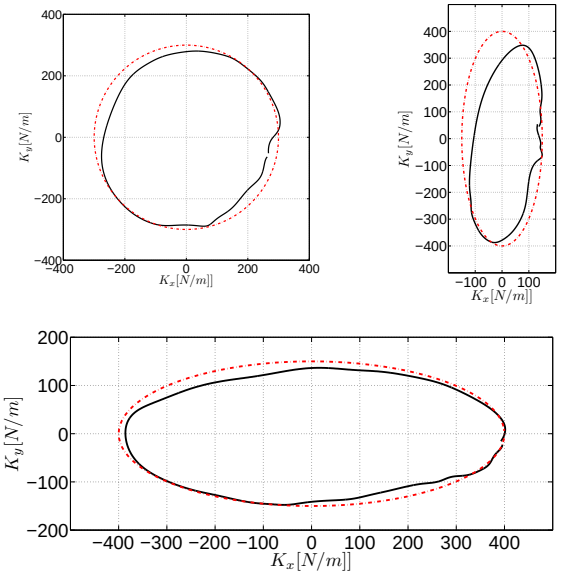

Fig. 8. Stiffness ellipse tracking in the x-y plane: desired stiffness ellipse (dashed line) and experimentally estimated stiffness ellipse by measured end-effector forces and positions (solid back line). The plots are relative to the set of parameters defined in Table I. Left: shape 1, Right: shape 2, Bottom: shape 3

constrained) is estimated to be around 10Hz. Subsequently, we described the implementation of an impedance controller to control the 3 DOF electro-hydraulically driven leg of HyQ. Preliminary results of simulations and experiments on the real robot are presented. Firstly, the feasibility of a full impedance law (Eq. 6) is assessed through simulation. Then, experimental data, obtained by a simpler implementation of the impedance controller (Eq. 8), shows that this controller is able to generate the desired Cartesian force vectors at the end effector. The end-effector forces are generated by hybrid actuators that act in concert. The implemented impedance controller shows a good tracking of the forces at the end-effector together with the capability to shape its stiffness behavior. This demonstrates the versatility and usefulness of this controller for future locomotion tasks, in which impacts are present and forces must be tracked at the end-effector to control robot dynamic stability.

Future work aims at completing the performance estimation of the HAA torque controller for different load conditions. We also plan to implement the full impedance controller with the use of a force sensor that will be attached at the foot. Our interests include also the extension of this controller to a full floating base system, setting for instance a desired impedance behavior on the COG of the robot. This may pose some challenges since, depending on the number of legs in contact with the ground, the COG Jacobian matrix will assume different dimensions. It may lead to torque discontinuities that must be carefully addressed. Last but not least, we will test our torque and impedance controllers in locomotion tasks in unstructured environments.

ACKNOWLEDGMENTS

This research has been funded by the Fondazione Istituto Italiano di Tecnologia.

REFERENCES

[1] A. Albu-Schäffer and G. Hirzinger. Cartesian impedance control techniques for torque controlled light-weight robots. In *Proceedings IEEE International Conference on Robotics and Automation (ICRA)*, volume 1, pages 657 – 663, 2002.

[2] T. Boaventura, C. Semini, J. Buchli, M. Frigerio, M. Focchi, and D.G. Caldwell. Dynamic locomotion of a torque-controlled quadruped robot. In *Proceedings IEEE International Conference on Robotics and Automation (ICRA)*, 2012. [Submitted].

[3] J. Buchli, M. Kalakrishnan, M. Mistry, P. Pastor, and S. Schaal. Compliant quadruped locomotion over rough terrain. In *Proceedings of the 2009 IEEE/RSJ International Conference on Intelligent Robots and Systems (IROS)*, pages 814–820, 2009.

[4] D.P. Ferris and C.T. Farley. Interaction of leg stiffness and surfaces stiffness during human hopping. *Journal of Applied Physiology*, 82(1):15–22, 1997.

[5] G. C. Goodwin, S. F. Graebe, and M. E. Salgado. *Control system design*. Prentice Hall, 2000.

[6] M. Görner, T. Wimböck, A. Baumann, M. Fuchs, T. Bahls, M. Grebenstein, C. Borst, J. Butterfass, and G. Hirzinger. The DLR-crawler: A testbed for actively compliant hexapod walking based on the fingers of DLR-Hand II. In *IEEE/RSJ International Conference on Intelligent Robots and Systems (IROS)*, pages 1525 –1531, sept. 2008.

[7] N. Hogan. Impedance control: An approach to manipulation: Part II – Implementation. *ASME, Transactions, Journal of Dynamic Systems, Measurement, and Control*, 107:8–16, 1985.

[8] MOOG Inc. *Data Sheet For E024 Series Microvalve*, 2003.

[9] J. Pratt, C.M. Chew, A. Torres, P. Dilworth, and G. Pratt. Virtual model control: An intuitive approach for bipedal locomotion. *The International Journal of Robotics Research*, 20(2):129–143, 2001.

[10] L. Sciavicco and B. Siciliano. *Modelling and Control of Robot Manipulators*. Springer, 2000.

[11] C. Semini. *HyQ - Design and Development of a Hydraulically Actuated Quadruped Robot*. PhD thesis, Italian Institute of Technology and University of Genoa, 2010.

[12] C. Semini, N.G. Tsagarakis, E. Guglielmino, M. Focchi, F. Cannella, and D.G. Caldwell. Design of HyQ - a hydraulically and electrically actuated quadruped robot. *IMechE Part I: J. of Systems and Control Engineering*, 225(6):831–849, 2011.

[13] S.A. Setiawan, J. Yamaguchi, Sang Ho Hyon, and A. Takanishi. Physical interaction between human and a bipedal humanoid robot-realization of human-follow walking. In *Proceedings. 1999 IEEE International Conference on Robotics and Automation, 1999.*, volume 1, pages 361 –367 vol.1, 1999.

[14] N. Tsagarakis, F. Becchi, L. Righetti, A. J. Ijspeert, and D. G. Caldwell. Lower body realization of the baby humanoid – iCub. In *Proceedings of the IEEE/RSJ International Conference on Intelligent Robots and Systems (IROS)*, pages 3616–3622, November 2007.